Academic Journal of Science and Technology
ISSN: 2771-3032 | Vol. 14, No. 1, 2025

Analysis and Recommendations on the Cause of Leakage Failure in CT90 Colied Tubing

Wenbin Wu, Jianliang Duan and Runqiu Gao

SHINDA(TANGSHAN) CREATIVE OIL & GAS EQUIPMENT CO..LTD, Tangshan 063000, China

Abstract: The CT90 coiled tubing experienced leakage during operation. This study aims to investigate the causes of tubing failure, improve its service life, and provide a reference for similar issues. The analysis includes the use of metallographic microscopy, optical microscopy, hardness testing, and other experimental methods to examine the metallographic structure, macro morphology, and hardness of the material. The findings reveal that during the pipeline's use, environmental factors led to brittleness, stress corrosion, crack formation, crack propagation, and subsequent leakage.

Keywords: Colied tubing; failure analysis; low carbon alloy steel.

1. Sample Information

Coiled tubing is made from high-strength low-carbon microalloy steel, which offers good strength and plasticity. Typically, a single length can reach several kilometers, and it is capable of undergoing multiple plastic deformations. Compared to traditional threaded connection pipes, coiled tubing is more convenient and faster to use during service, offering greater safety and reliability.[1]

SHINDA (TANGSHAN) CREATIVE OIL & GAS EQUIPMENT CO., LTD. produced a coiled tubing disc with a diameter of φ44.5×4.0 CT90 and a length of 5500 meters. The tubing experienced a first break after passing through the gooseneck during winding onto the reel and a second break in the wellbore. The treatment involved using 18% HCl with an inhibitor (SCA-2000P) in a total volume of 4m³, with the inhibitor mixed at a ratio of 2 liters per 1m³. The acid remained in contact with the tubing for approximately 3 hours.

The collapse occurred in two areas near the biased welds. According to feedback from the job site, the coiled tubing was lifted, and a break occurred between the gooseneck and the reel pipe. Approximately 900-1000 meters of the tubing were left in the well. The tubing was then pulled up, but the second break occurred at the next biased weld. Approximately 400 meters of tubing, along with the tools, are still stuck in the well.

The broken tubing was labeled as A1, while the remaining intact tubing was labeled as A2 for analysis. The overall macroscopic fracture morphology shows a brittle fracture with no significant plastic deformation[2], as shown in the figure 1.

Figure 1. Sample information

2. Test Methods and Results

2.1. Chemical composition analysis

According to ASTM A751-2021, chemical composition analysis was conducted using the Labspark 1000 direct reading spectrometer. The results of the analysis are presented in Table 1. Based on the analysis, it can be concluded that the chemical composition of the sample meets the specified technical requirements.

Table 1. Chemical composition test results

Sample number	Element content (wt%)										
	C	Si	Mn	P	S	Cu	Ni	Cr	Mo	Nb	Ti
A1	0.160	0.368	0.857	0.010	0.001	0.234	0.111	0.542	0.173	0.017	0.021
A2	0.160	0.363	0.844	0.010	0.002	0.234	0.119	0.541	0.171	0.017	0.021
Technical requirements	≤0.16	≤0.50	≤1.20	≤0.020	≤0.005	/	/	/	/	/	/

2.2. Dimension measurement

The outer diameter and wall thickness of the unbroken ends of A1 and A2 tubes were tested along the axis at the positions indicated in A-A, B-B, C-C, and D-D. The results are presented in Table 2 below. The findings indicate that the wall thickness has been reduced compared to the shipped size of the finished tube.

Table 2. Dimensional measurement result

Measuring position	A-A	B-B	C-C	D-D	t1	t2	t3	t4
A1/mm	44.50	44.45	44.51	44.46	3.974	4.017	4.015	4.057
A2/mm	43.92	44.06	43.96	43.97	3.693	3.699	3.817	3.846
Acceptance standard/mm	44.25~44.75				3.8~4.3			

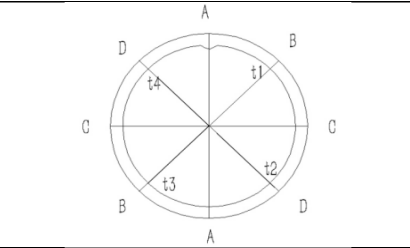

2.3. Metallographic analysis of tube cross section near fracture location

A section of tubing near the fractures of A1 and A2 was cut off for analysis. For both A1 and A2, grain size analysis was conducted using the YJ-2000 metallographic microscope and image analysis system, in accordance with ASTM E112-2013 standards. The results are shown in Table 3. The findings indicate that the grain size of the samples meets the technical requirements. There was no significant microstructural difference between the weld and biased weld areas. However, pitting was observed on the tube, and the microstructure revealed clear gaps between the grains, which exhibit the typical microscopic morphology of hydrogen-induced cracking.[3]

Table 3. Results of grain size rating

A1	grain size	A2	grain size
Weld	10.5	Weld	10.5
Bias weld	10.5	Bias weld	10.5
Base material	11.0	Base material	11.0
standard request	≥8	standard request	≥8

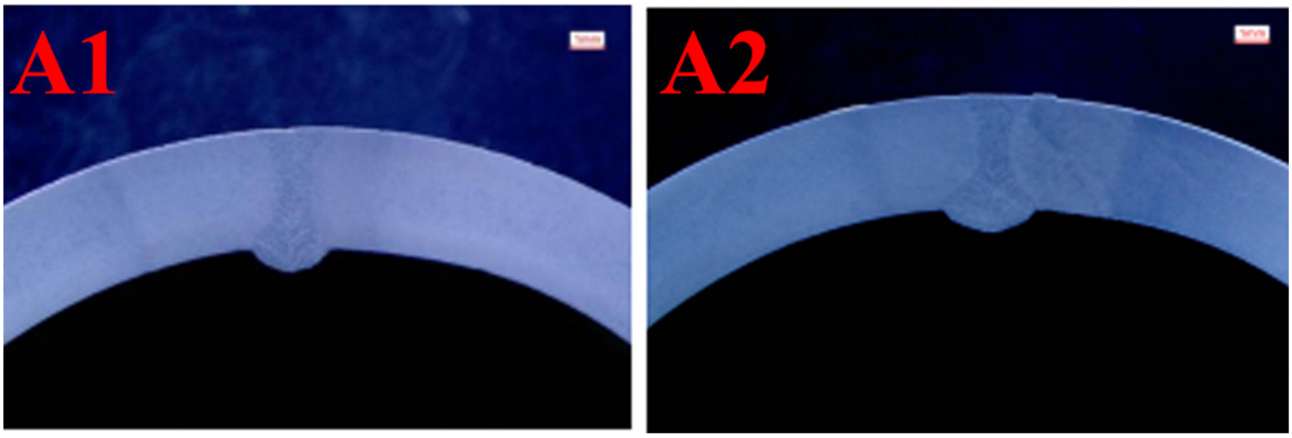

Figure 2. Macroscopic surface of metallographic corrosion 6.8X

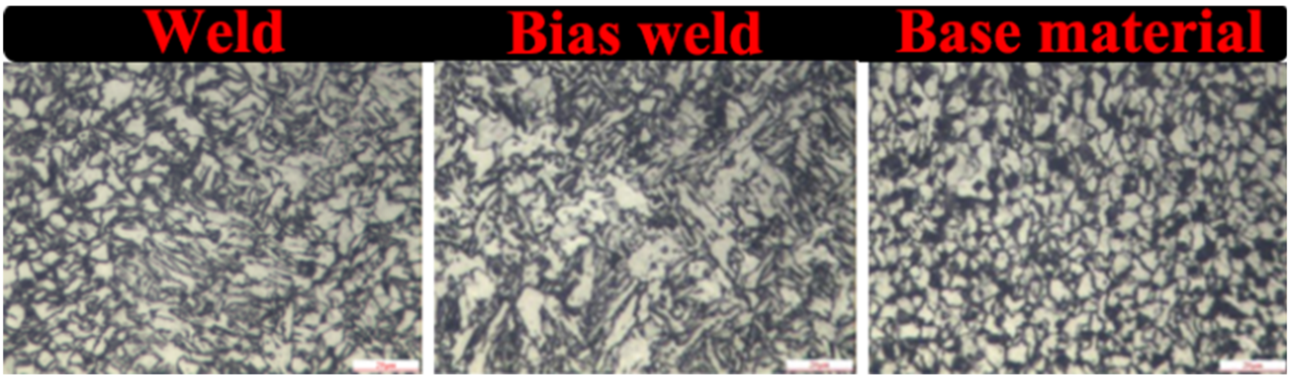

Figure 3. Metallographic analysis for A1(500X)

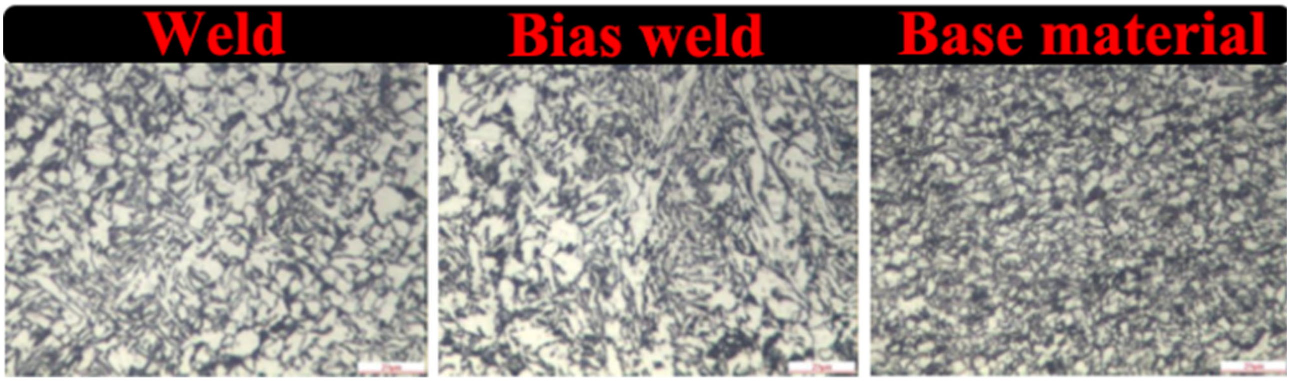

Figure 3. Metallographic analysis for A2(500X)

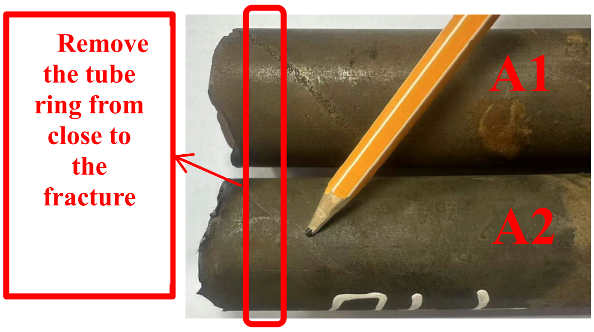

Figure 4. Sampling point

2.4. Hardness testing of tube cross section near fracture location

A section of tubing near the fractures of A1 and A2 was cut off for hardness testing. For both A1 and A2, the 200HVS-5 digital display small-load Vickers hardness tester was used to perform the hardness test in accordance with ASTM E384-22 standards, with hardness conversion performed as per ASTM E140-2012b (2019) e1. The hardness test positions on the original tube are shown in Figure 5[4], and the data are presented in Table 4. The results indicate that the hardness values meet the technical requirements, and the hardness is consistent across the tested areas.

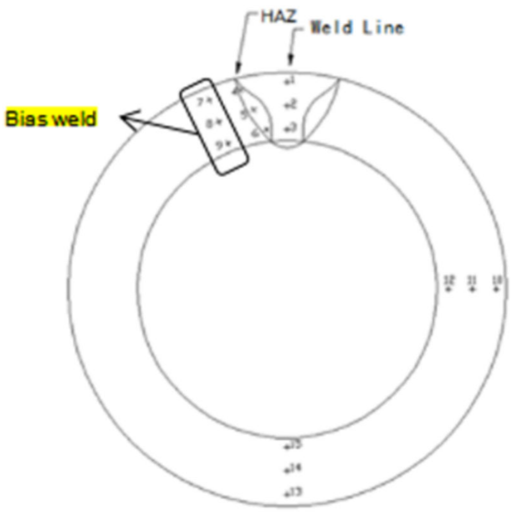

Figure 5. Through-wall Hardness Test Impression Location

Table 4. Hardness test result

Sample	Weld line			HAZ			Bias weld			90°zone			180°zone		
	1	2	3	4	5	6	7	8	9	10	11	12	13	14	15
A1 Measured value	100	100	100	98.5	98.5	98.0	99.0	100	100	100	100	99.5	100	100	100
Average	100HRB			98.5HRB			100HRB			100HRB			100HRB		
A2Measured value	100	100	100	97.5	97.0	97.5	98.5	100	99.0	100	100	100	100	100	100
Average	100HRB			97.5HRB			99.0HRB			100HRB			100HRB		
Test Requirement	≤22HRC (248HV)														
	Below 20 HRC, HRB is used														

2.5. Metallographic analysis of bias weld

The area of the A1 and A2 tubes containing the injury was sampled for analysis. Grain size analysis was conducted using the YJ-2000 metallographic microscope and image analysis system, in accordance with ASTM E112-2013 standards. The results are presented in Table 5. The findings indicate that the grain size of the sample meets the technical requirements and is similar to the metallographic structure of the tube cross-section. However, the microstructure reveals clear gaps between the grains, exhibiting the typical microscopic morphology of hydrogen-induced cracking.

Table 5 Results of grain size rating

A1	grain size	A2	grain size
Bias weld	10.5	Base material	10.0
standard request	≥8	standard request	≥8

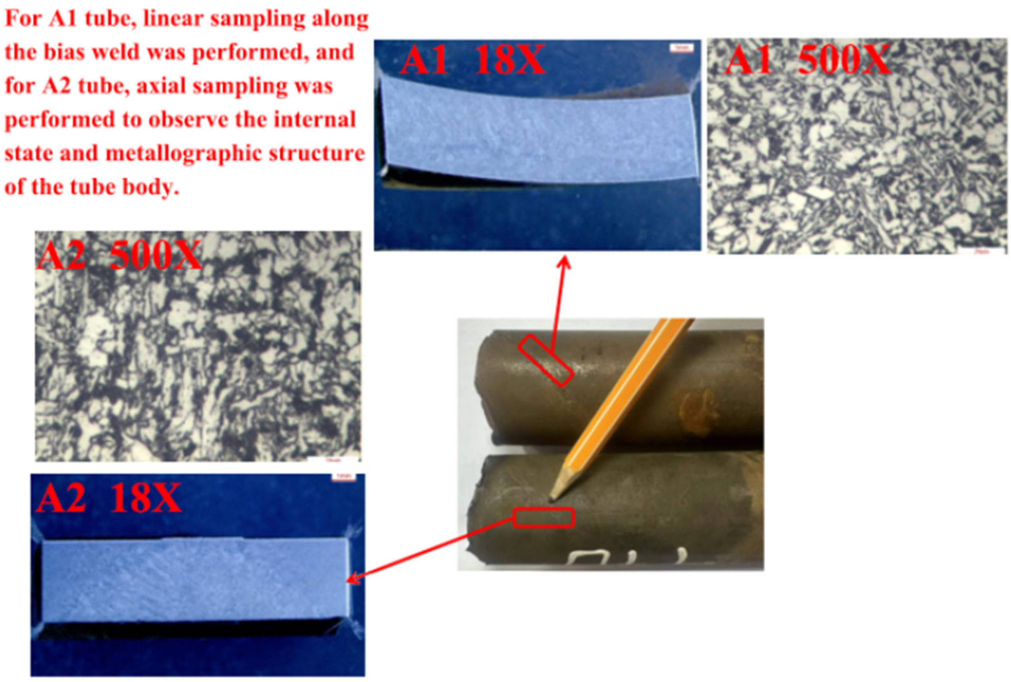

Figure 6. Metallographic analysis of bias weld

2.6. Hardness testing of bias weld

Hardness tests for the A1 and A2 biased weld and base material were performed using the 200HVS-5 digital display small-load Vickers hardness tester, in accordance with ASTM E384-22 standards. Hardness conversion was carried out based on ASTM E140-2012b (2019) e1. The results are presented in Table 7. The hardness data meet the technical requirements, and the hardness is uniform across the samples.

Table 6. Results of grain size rating

A1	location-1	location-2	location-3
Measured value	100.0HRB	99.0HRB	99.5HRB
A2	location-1	location-2	location-3
Measured value	100.0HRB	99.0HRB	99.0RB
Test Requirement	≤22HRC (248HV)		
	Below 20 HRC, HRB is used		

3. Interpretation of Result

Hydrogen atoms, with the smallest atomic radius, can easily diffuse into metals such as steel and copper, a phenomenon commonly observed in H_2S oil wells. In the oil and gas, as well as the petrochemical industries, when carbon steel or low alloy steel is used in a wet H_2S environment, the material is prone to severe embrittlement.[5]

Hydrogen atoms infiltrate the gaps between metal grains and, over time, diffuse deeper into the material. While hydrogen diffusion at room temperature is relatively slow, its solubility in steel increases with temperature, causing hydrogen to diffuse toward stress concentration sites. At these sites, hydrogen molecules form and generate significant pressure. This pressure is influenced by both the residual stress within the material and the external stress applied. When this resultant force exceeds the yield strength of the material, fracture occurs.

(1) **Hydrogen Induced Cracking (HIC)**

HIC can occur and propagate within steel without the application of external stress.

(2) **Sulfide Stress Cracking (SSC)**

SSC primarily occurs in areas with high hardness, such as the weld zone and the biased weld.

Since hydrogen embrittlement is driven by the diffusion of hydrogen atoms, and diffusion depends on factors such as the concentration gradient, temperature, and material type, hydrogen embrittlement typically results in delayed fracture.

In summary, the tube that experienced failure shows no abnormality in the morphology and structure of the biased weld. However, the microstructure reveals clear gaps between the grains, indicative of hydrogen-induced cracking. The fracture of the tube can be attributed to the combined effects of HIC and SSC in the hydrogen sulfide well environment.[6]

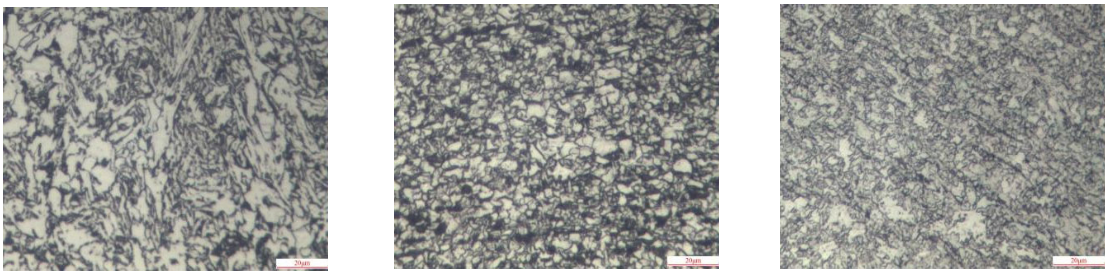

Bias weld 500X of problem tube **Base material 500X of problem tube** **Base material 500X of conventional CT90**

Figure 7. Comparison of microstructure of different samples

Note: It can be observed that the grain gaps in both the biased weld and the base material microstructure are larger than those in conventional CT90. This suggests the possibility that hydrogen atoms may accumulate in the grain interstitial spaces, causing these gaps to expand.

Bias weld 18X of problem tube **Weld 18X of A2 problem tube**

Figure 8. Macroscopic surface of metallographic corrosion 6.8X

Note: It is observed that the grain gaps in both the biased weld and the base material microstructure are larger compared to conventional CT90. This indicates the possibility that hydrogen atoms may accumulate in the interstitial spaces between grains, causing these gaps to widen.

Acknowledgements

Central Government's Guidance for Local Science and Technology Development Fund Project (Science and Technology Achievements Transfer and Transformation Project) No.236Z1022G.

References

[1] Bi, Z.Y.(2012).Advances in CoiledTubing and lts Application Technology*Welded Pipe*,*35*(9),5-12.DO1:10.19291/i.cnki.1001-3938.2012.09.001

[2] Qiao Lingyun, Li Bofeng, Yan Jixuan, et al. Analysis of Leakage Failure of 110 ksi Grade Coiled Tubing[J]. Welded Pipe and Tube, 2020, 43(03): 45 - 49. DOI: 10.19291/j.cnki.1001 - 3938.2020.03.009

[3] Zhang, F.; Li, J.; Zhu, H.; Jing, C.; Wang, B.; Qi, Y. Study on Variable Stress Corrosion Susceptibility of Four Typical High-Strength Sucker Rods in High-Salinity Well Fluids. [J].*Processes* **2023**, *11*(9), 2762. https://doi.org/10.3390/PR11092762.

[4] Kawakami, R.; Saeki, R.; Munetoh, S.; Ohgai, T. Micro-Vickers Hardness of Cu and Cu_2O Dual Phase Composite Films Electrodeposited from Acidic Aqueous Solutions Containing Polyethylene Glycol[J].Crystals 2023, 13(12), 1654. https://doi.org/10.3390/CRYST13121654.

[5] Zhang, P.; Majid, L.; Anthony, E. H.; Marceau, R. K. W.; Hilditch, T.; Tan, M. Y. Effect of Microstructure on Hydrogen Embrittlement and Hydrogen-Induced Cracking Behaviour of a High-Strength Pipeline Steel Weldment[J]Corrosion Science 2024, 227, 111764.https://doi.org/10.1016/J.CORSCI.2023.111764.

[6] Oh, S. B.; Choi, Y.; Shin, E. J.; Seong, B. S. Effect of Hydrogen on HIC and SSC Behaviors of Line Pipe Steels[J]. Proceedings of the Korean Society of Surface Engineering 2013, 556-556.